

A Universal Nucleoside with Strong Two-Band Switchable Fluorescence and Sensitivity to the Environment for Investigating DNA Interactions

Dmytro Dziuba,[†] Viktoriia Y. Postupalenko,[‡] Marie Spadafora,[†] Andrey S. Klymchenko,[‡] Vincent Guérineau,[§] Yves Mély,[‡] Rachid Benhida,^{*,†} and Alain Burger^{*,†}

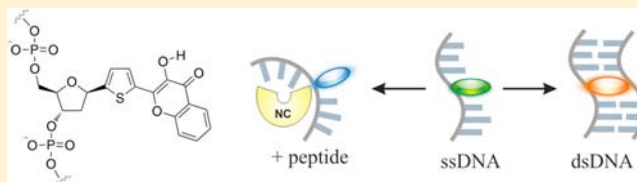
[†]Institut de Chimie de Nice, UMR 7272, Université de Nice Sophia Antipolis, CNRS, Parc Valrose, 06108 Nice cedex 2, France

[‡]Laboratoire de Biophotonique et Pharmacologie, UMR 7213, Faculté de Pharmacie, Université de Strasbourg, CNRS, 74 Route du Rhin, 67401 Illkirch, France

[§]Centre de recherche de Gif, Institut de Chimie des Substances Naturelles CNRS, Avenue de la Terrasse, 91198 Gif-sur-Yvette Cedex, France

Supporting Information

ABSTRACT: With the aim of developing a new tool to investigate DNA interactions, a nucleoside analogue incorporating a 3-hydroxychromone (3HC) fluorophore as a nucleobase mimic was synthesized and incorporated into oligonucleotide chains. In comparison with existing fluorescent nucleoside analogues, this dye features exceptional environmental sensitivity switching between two well-resolved fluorescence bands. In labeled DNA, this nucleoside analogue does not alter the duplex conformation and exhibits a high fluorescence quantum yield. This probe is up to 50-fold brighter than 2-aminopurine, the fluorescent nucleoside standard. Moreover, the dual emission is highly sensitive to the polarity of the environment; thus, a strong shielding effect of the flanking bases from water was observed. With this nucleoside, the effect of a viral chaperone protein on DNA base stacking was site-selectively monitored.



INTRODUCTION

Designing DNA-based fluorescent structures with site-specific responses to intermolecular interactions is a great challenge. The majority of environmentally sensitive fluorescent nucleosides are single-band emitters that respond to environmental changes by changes in the fluorescence intensity or a shift in the emission maximum.¹ These nucleosides suffer from limitations such as quenching by neighboring nucleobases or poor sensitivity to perturbations in the DNA structure. For example, 2-aminopurine (2-AP), the most popular nucleotide mimic,^{1b} is used as an intensimetric probe but exhibits low sensitivity to the environment and low quantum yields in DNA duplexes.² These drawbacks have stimulated further research combining top achievements in photophysics, spectroscopy, and synthetic chemistry.^{1b} It is particularly important that the spectrum of the artificial nucleobase be highly sensitive to intermolecular interactions. Ideally, a single dye should be employed to avoid double labeling that is needed for fluorescence resonance energy transfer (FRET), excimers, or J-aggregates.³ In addition, the effect of the nucleotide mimic on the double-helical structure of native DNA must be minimal.

Therefore, we addressed the unique photophysical properties of 3-hydroxychromone (3HC) dyes, which exhibit polarity- and hydration-sensitive switching between well-resolved highly intense fluorescence bands in the visible range. As a result of excited-state intramolecular proton transfer (ESIPT), these

fluorophores exhibit two excited states: the initially excited normal form (N*) and the tautomeric form (T*); each form generates one well-resolved emission band (Figure 1).⁴

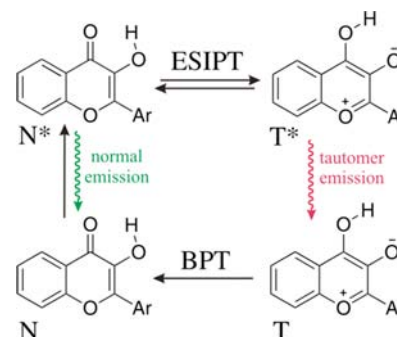


Figure 1. ESIPT reaction in 3-hydroxychromones. BPT denotes back proton transfer, and N* and T* represent the normal and tautomeric emissive forms, respectively.

The dual emission of 3HCs is highly sensitive to the environment because an increase in the donating ability of the hydrogen bond and the dielectric constant of the solvent inhibit

Received: March 30, 2012

Published: May 16, 2012

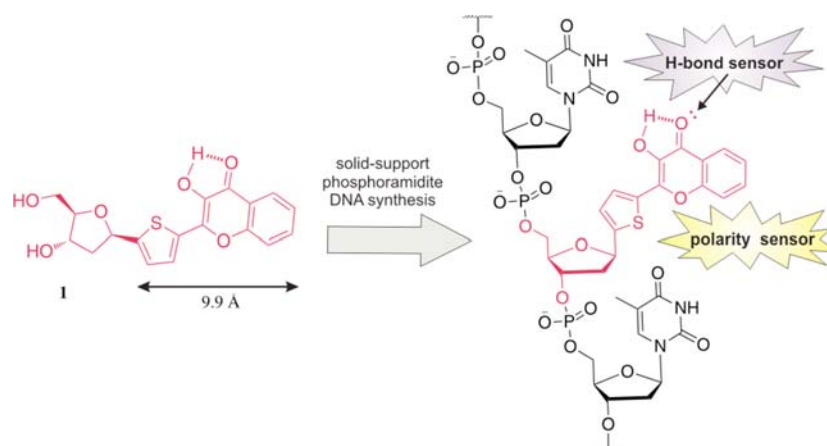


Figure 2. Hydrogen-bonding- and dielectric-constant-sensitive nucleoside **1** bearing 2-thienyl-3-hydroxychromone as a base surrogate and its incorporation into DNA.

Table 1. Thermal Denaturation of Double-Stranded ODN Samples

entry	dsDNA ^a	T _m (°C)	ΔT _m (°C)	entry	dsDNA ^a	T _m (°C)	ΔT _m (°C)	entry	dsDNA ^a	T _m (°C)	ΔT _m (°C)
1	AAA + TTT	50.6	0	12	TAT + ATA	50.8	0	22	CAC + GTG	55.1	0
2	AAA + TAT	39.2	-11.4	13	TAT + AAA	42.1	-8.7	23	CAC + GAG	45.8	-9.3
3	AAA + TGT	40.7	-9.9	14	TAT + AGA	42.8	-8	24	CAC + GGG	50.3	-8.8
4	AAA + TCT	39.8	-10.8	15	TAT + ACA	40.9	-9.9	25	CAC + GCG	47.2	-7.9
5	AAA + TAbT	33.7	-16.9	16	TAT + AAbA	33.1	-17.7	26	CAC + GAbG	40.5	-14.6
6	AMA + TTT	41.4	-9.2	17	TMT + ATA	45.8	-5	27	CMC + GTG	48.9	-6.2
7	AMA + TAT	41.2	-9.4	18	TMT + AAA	46.3	-4.5	28	CMC + GAG	49.9	-5.2
8	AMA + TGT	41.4	-9.2	19	TMT + AGA	45.3	-5.5	29	CMC + GGG	50.0	-5.1
9	AMA + TCT	43.1	-7.5	20	TMT + ACA	46.5	-4.3	30	CMC + GCG	51.5	-3.6
10	AMA + TAbT	41.0	-9.6	21	TMT + AAbA	46.6	-4.2	31	CMC + GAbG	51.3	-3.8
11	M-TAT + ATA	55.5	+4.7								

^aIn pH 7 buffer (10 mM cacodylate, 150 mM NaCl).

the ESIPT reaction and thus decrease the relative intensity of the T* band.⁵ A critical advantage of ratiometric dyes over conventional single-band dyes is that this ratio depends only on the microenvironment of the fluorophore and not on the local concentration of the dye or the instrument settings. In addition to the ratio of the two emission bands, information could also be extracted from the positions of the absorption and two emission maxima.⁶ 3HCs have been shown to be powerful fluorescent tools to probe lipid bilayers, cell membranes, proteins, and peptides,⁷ but the synthesis of DNA labeled with ratiometric 3HC derivatives and their application for sensing have never been described. Our strategy relies on a thienyl-3HC-modified deoxyribose **1** that allows their incorporation into oligonucleotides (ODNs) (Figure 2).

We previously described the synthesis and photophysical properties of such nucleoside analogues.⁸ Derivative **1** displays the most promising photophysical properties as a polarity- and hydration-sensitive label for incorporation into ODNs. The thienyl-3HC group of **1** is an attractive analogue of nucleic bases because it is a flat molecule and its size corresponds well to the size of the two complementary AT and GC base pairs. We preferred to graft the dye to deoxyribose at the thienyl substituent rather than to the benzene ring of the chromone. This grafting should favor the exposure of the 4-carbonyl moiety to local water in singly labeled ODNs (Figure 2). Annealing with complementary ODNs or formation of a protein–DNA complex should reduce the local hydration and polarity of the dye and thus change the ratio of the intensities of

the two emission bands of **1**. Herein we report the synthesis of ODNs incorporating **1**, the photophysical properties of the labeled ODNs, and the ability of **1** to sense the DNA microenvironment and DNA–protein interactions site-selectively.

RESULTS AND DISCUSSION

The syntheses of the phosphoramidite of **1** and the labeled 15- and 16-mer ODNs is described in the Supporting Information. The 15-mer d(CGT TTT XMX TTT TGC) and 16-mer 5'-d(M CGT TTT TAT TTT TGC) sequences containing thienylchromone **1** at the positions labeled M were chosen as model sequences to characterize the photophysical properties of **1** in ODNs. In the 15-mers (AMA, TMT, CMC and GMG), **1** was incorporated in the middle of the sequence where the influence of the nucleoside analogue on the thermal stability should be the most pronounced. Moreover, the sequences differed by the residues flanking the modified nucleotide to compare the properties of label **1** in different ODN contexts. In the 16-mer (M-TAT), the ODN contained a dangling **1** at the 5' end.⁹ Control experiments were conducted with reference wild-type strands of composition d(CGT TTT XAX TTT TGC), where X = A, C, G or T. Each ODN was then annealed with its complementary ODN (noted in italics) containing a natural base or an abasic site located at the position opposite dye **1**, resulting in duplexes with different compositions (see Table S1 in the Supporting Information). The sequences of the complementary strands were d(GCA AAA YXY AAA ACG), in

which Y is A, C, G, or T and X is any of the natural bases or an abasic site (*Ab*).

As a first step to characterize the ODNs containing thienylchromone **1**, the thermodynamic stabilities of their duplexes were compared with the stabilities of the corresponding unlabeled duplexes by monitoring the temperature-induced absorbance changes at 260 nm (Table 1 and Figure S4 in the Supporting Information). Thermal denaturation studies showed that incorporation of nucleoside analogue **1** opposite a natural base or an abasic site led to duplexes with comparable thermal stabilities (entries 6–10, 17–21, and 27–31). Although less stable than the corresponding fully canonical duplexes, those containing **1** are more stable than the nonlabeled duplexes with mismatches (Table 1). For example, the duplexes containing the natural pair (TAT + ATA), the mismatched pair (TAT + AAA), and dye **1** (TMT + ATA) melted with T_m values of 50.8, 42.1, and 45.8 °C, respectively (entries 12, 13, and 17). The data indicate that the dye stacks more strongly than the natural bases, likely as a result of a larger area of contact with the surrounding bases. A similar effect was observed in previous studies with labeled ODNs containing aromatic groups (e.g., pyrene, biphenyl, bipyridine, isoquinoline) instead of the natural base.¹⁰ Thus, since thienyl-3HC **1** is nondiscriminating toward natural bases and less destabilizing than a mismatch, thienyl-3HC shows characteristics of a universal base.¹¹ Relative to the canonical duplexes, TMT + AXA and CMC + GXG gave smaller differences in T_m (ΔT_m) than the AMA + TXT duplexes (Table 1). The ΔT_m values can be grouped in two sets. One is in the range of 3.6–6.2 °C, and the other has values of 7.5–9.4 °C. The more favorable ΔT_m values for the TMT + AXA and CMC + GXG duplexes might be due to an increased overlap between the chromone moiety and the flanking purines of the complementary strand, as proposed for ODNs incorporating hydroxyphenylbenzoxazole.¹² Furthermore, in comparison to the natural base adenine, **1** enhanced the T_m of duplexes containing an abasic site by ~7 °C for AMA + TABT and 11–13 °C for TMT + AAbA and CMC + GAbG (Table 1). The stacking ability of dye **1** was further confirmed by the 4.7 °C increase in T_m observed for the M-TAT + ATA duplex containing the dangling thienyl-3HC (Table 1).⁹

In a second step, the influence of **1** on the secondary structure of the labeled duplexes was studied by circular dichroism (CD) spectroscopy (Figure S5 in the Supporting Information). The CD spectra were similar to those of the unlabeled duplexes, indicating that the dye does not affect the B-helix conformation of the duplexes. Altogether, the thermal denaturation and CD data support the idea that thienyl-3HC **1** can replace any natural nucleobase or base pair, giving stable duplexes with the B conformation.

In a third step, we characterized the UV absorbance and fluorescence properties of **1** in the 15- and 16-mer ODNs, either in their single-stranded (ss) or double-stranded (ds) states (Table 2 and Figure 3). In buffer, labeled ssODNs and dsODNs showed absorption bands centered at 373–376 and 372–381 nm, respectively. The absorption maxima of the labeled ssODNs and dsODNs were red-shifted by 5–14 nm relative to that of the free dye in buffer, suggesting stacking of the dye with its flanking bases (Table 2 and Figure S6 in the Supporting Information). A red shift of the absorption maximum is commonly observed with intercalating dyes (e.g., acridine and phenanthridinium).¹³ In ssODNs, the effect of flanking bases on the 3HC absorption maximum was larger

Table 2. Spectroscopic Data for Nucleoside **1** and Labeled ODNs

entry	sample ^a	λ_{abs}^b (nm)	$\lambda_{\text{N}^*}^c$ (nm)	$\lambda_{\text{T}^*}^d$ (nm)	$I_{\text{N}^*}/I_{\text{T}^*}^e$	QY (%) ^f
1	1 ^g	367	440	515	1.72	4.6
2	AMA	376	440	541	0.11	17
3	AMA + TTT	376	441	540	0.17	24
4	AMA + TAT	376	439	542	0.09	20
5	AMA + TGT	375	439	542	0.10	16
6	AMA + TCT	376	438	543	0.09	25
7	AMA + TABT	377	437	542	0.07	30
8	TMT	373	435	540	0.23	14
9	TMT + ATA	373	437	540	0.14	38
10	TMT + AAA	376	434	540	0.07	28
11	TMT + AGA	373	433	541	0.09	13
12	TMT + ACA	373	433	540	0.07	30
13	TMT + AAbA	373	433	541	0.08	35
14	CMC	373	434	543	0.28	4
15	CMC + GTG	375	434	540	0.41	1
16	CMC + GAG	381	429	519	0.10	2
17	CMC + GGG	373	433	540	0.43	1
18	CMC + GCG	375	434	540	0.45	1
19	CMC + GAbG	375	433	540	0.39	1
20	GMG	374	433	541	0.66	2
21	M-TAT	374	438	542	0.59	8
22	M-TAT + ATA	372	437	532	1.05	1

^aIn pH 7 buffer (10 mM cacodylate, 150 mM NaCl). ^b λ_{abs} is the position of the absorption maximum. ^c λ_{N^*} is the position of the fluorescence maximum of the N* band. ^d λ_{T^*} is the position of the fluorescence maximum of the T* band. ^e $I_{\text{N}^*}/I_{\text{T}^*}$ is the ratio of the intensities of the two emission bands at their maxima. ^fQY is the fluorescence quantum yield calculated using quinine sulfate (QY = 0.577 in 0.5 M H₂SO₄) as a reference. ^gData taken from ref 8, where a pH 6.5 buffer (10 mM phosphate) was used.

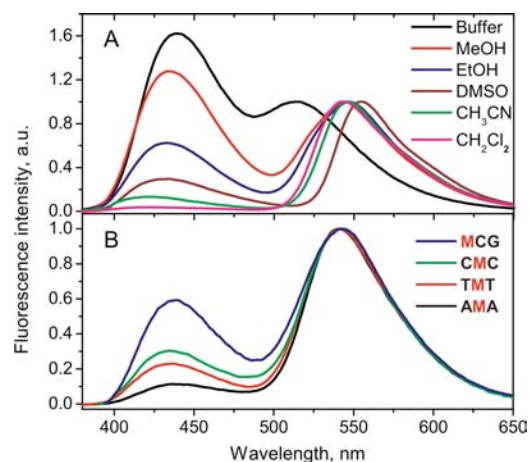


Figure 3. Normalized fluorescence spectra of (A) free thienyl-3HC **1** in different solvents⁸ and (B) labeled ssODNs in pH 7 buffer (10 mM cacodylate, 150 mM NaCl).

with purines than pyrimidines, suggesting a stronger stacking with purines because of their larger size.

The labeled ODNs showed well-resolved two-band emission, with the short- and long-wavelength maxima centered at 429–441 and 519–543 nm, respectively (Table 2). These values are very close to those obtained for free **1** in various organic solvents (Figure 3). Thus, the short- and long-wavelength

bands were assigned to the emissions of the N^* and T^* forms, respectively, indicating that the 3HC dye still undergoes an ESIPT reaction in ODNs and therefore maintains its fundamental properties. The Stokes shifts for the first and second emission bands were ~ 3870 and ~ 8100 cm^{-1} , respectively. The large Stokes shift obtained for the second emission band is typical for ESIPT probes.

Interestingly, the fluorescence quantum yield (QY) of the dye in single- and double-stranded ODNs varied from 1 to 38% depending on the surrounding nucleobases (Table 2). In ODNs with A or T flanking the dye, the quantum yields of the ss and ds forms (entries 2–13) were 3–8-fold larger than that of the free dye **1** in buffer.

Moreover, with the exception of G opposite **1** (Table 2, entries 5 and 11), the quantum yields were higher in duplexes than in single strands and superior to the highest value determined for free **1** in aprotic solvents (QY = 20% in dimethyl sulfoxide).⁸ These observations are consistent with the dye being shielded in the duplex, with reduced quenching by the solvent. In addition, reduced flexibility and/or rotation around the single bond between the chromone and thienyl moieties might also contribute to the higher quantum yield, as proposed for thiazole orange, green fluorescent protein (GFP)-like, and uracil-containing pyridine fluorophores.¹⁴ The quantum yields in ODNs with C or G flanking the dye were lower (entries 14–22). The decrease in quantum yield in duplexes with G opposite **1** confirmed the propensity of G to quench the dye (Table 2, entries 5, 11, and 17). Quenching of fluorescent nucleoside analogues in ODNs is common.^{1b} For example, G, T, and C efficiently quench pyrene,¹⁵ while 2-AP is quenched by all four natural nucleobases.² Importantly, the fluorescence quantum yield of **1** is 2–25-fold larger than that of 2-AP in corresponding ODN sequences.¹⁶ In addition, the molar absorptivity of **1** ($13\,000\text{ M}^{-1}\text{ cm}^{-1}$) is about twice that of 2-AP ($7200\text{ M}^{-1}\text{ cm}^{-1}$), which makes it up to 50-fold brighter.^{8,16}

In comparison to free dye **1** in buffer, the labeled ODNs showed a strong decrease in the N^*/T^* intensity ratio (I_{N^*}/I_{T^*}) together with blue and red shifts of the N^* and T^* bands, respectively (Table 2 and Figure 3). For most of the labeled ODNs, I_{N^*}/I_{T^*} was between those for the free dye in dichloromethane and acetonitrile (Figure 3), indicating that the environment of the labeling site is mainly aprotic and of medium polarity.⁸ Here we compared only ODNs showing sufficient fluorescence quantum yields ($\geq 4\%$; entries 2–14). In ssODNs, I_{N^*}/I_{T^*} varied strongly with the nature of the neighboring bases. TMT and CMC showed larger I_{N^*}/I_{T^*} than AMA, likely as a consequence of more efficient stacking of dye **1** with purines and thus more efficient shielding from water. These results are consistent with the UV spectroscopy data, where the more pronounced red shift of the 3HC absorption maximum was observed with flanking adenines in AMA (see above). In dsODNs, I_{N^*}/I_{T^*} rather uniformly showed lower values, with the exception of T opposite **1** in both the AMA and TMT duplexes (entries 3 and 9). It is clear that in dsDNA, the environment of **1** is highly dehydrated, which explains the low I_{N^*}/I_{T^*} values. The anomalous effect of having T opposite **1** could be explained by H-bonding between this base and the 4-carbonyl of **1**, which would hamper the ESIPT and increase I_{N^*}/I_{T^*} . Finally the highest N^*/T^* intensity ratio was observed for M-TAT ssDNA, where dye **1**, located at the 5' end, is more exposed to water. Thus, both the fluorescence quantum yield and I_{N^*}/I_{T^*} for thienyl-3HC

dye **1** show high sensitivity to the neighboring bases, which is a unique feature with respect to the existing fluorescent bases.^{1b}

Furthermore, the photostabilities of nucleoside **1** and its ssODN in buffer were comparable to that of prodan in ethanol, whereas for the corresponding dsODN the photostability was remarkably higher (Figure S7 in the Supporting Information).

Finally, to validate the application of the new fluorescent base as a probe for sensing biomolecular interactions, we studied the interaction of the labeled ODNs with the HIV-1 nucleocapsid protein (NC). This nucleic acid chaperone protein can locally destabilize ssODNs or hairpins through interactions with the hydrophobic amino acids of its folded zinc finger motifs.¹⁷ Addition of NC to ssODNs (AMA, TMT, and CMC) significantly increased their N^*/T^* intensity ratios, showing a 1:1 interaction stoichiometry (Figure 4 and Figure S8 in the Supporting Information).

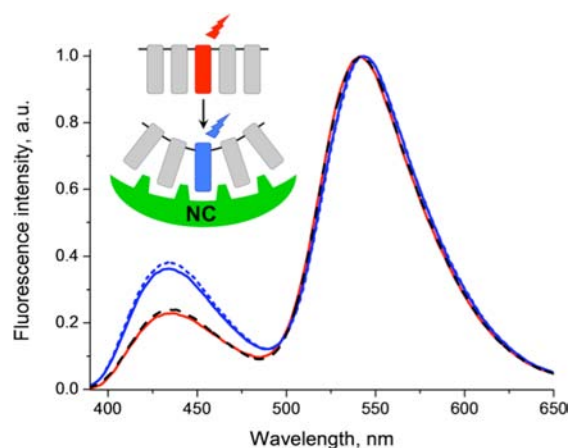


Figure 4. Fluorescence spectra of the TMT ODN in the absence (red) or presence of 1 equiv (blue solid) or 3 equiv (blue dotted) of NC or 3 equiv of NC-SSHS (black dashed) peptides. The spectra were normalized at the T^* band. The experiments were performed in pH 7 buffer (10 mM cacodylate, 150 mM NaCl). Binding of the NC peptide to the labeled ODN leads to an increase in I_{N^*}/I_{T^*} due to the insertion of the hydrophobic amino acids of its folded finger motifs between the bases.

As already described for several other NC–ODN complexes, these observations suggest that intercalation of the zinc finger residues between the bases of these labeled ssODNs, at the level of **1**, decreases the base stacking and increases the exposure of the bases to water.¹⁸ In contrast, no change in the probe signal was observed upon interaction of NC with the labeled dsODNs (data not shown) because of the limited destabilizing effect of NC on stable ds regions.¹⁹ Moreover, a nonfolded mutant of NC (NC-SSHS) that binds ssODNs only through electrostatic interactions with the ODN phosphate groups^{18a,20} induced no change in the emission spectra of the labeled ODN sequences (Figure 4). These data confirmed that, in contrast to NC, the NC-SSHS mutant does not affect the base stacking in ssODNs. Thus, our new fluorescent base allows site-selective monitoring of subtle conformational changes produced by interacting proteins.

CONCLUSION

ODNs incorporating the two-band fluorescent thienyl-3HC **1** were successfully synthesized. Dye **1** can replace any natural nucleobase or base pair to form duplexes with the B

conformation having nearly the same stability as the native unlabeled duplex. Thus, **1** possesses the characteristics of a universal base. In comparison to the “gold standard” 2-AP, the new base is up to 50-fold brighter, and its absorption is red-shifted by 60 nm. Consequently, the absorption of the new base does not overlap with the intrinsic absorptions of nucleic acids and proteins. The new fluorescent base demonstrates all the advantages of wavelength ratiometric detection, including a large separation between the emissions of the two bands and a dramatic variation of their relative contributions. Moreover, the high sensitivity of the dual emission of **1** to the polarity of the environment induces a strong shielding effect of the flanking bases from water. Finally, the new base was successfully applied to monitor local conformational changes of ssODNs upon interaction with the viral nucleocapsid protein. Therefore, the new base appears to be a new universal tool for DNA research. Further chemical modifications of 3HC nucleobases will provide new possibilities to tune and improve their properties.

■ ASSOCIATED CONTENT

📄 Supporting Information

Experimental procedures, analytical data, and spectra. This material is available free of charge via the Internet at <http://pubs.acs.org>.

■ AUTHOR INFORMATION

Corresponding Author

rachid.benhida@unice.fr; burger@unice.fr

Notes

The authors declare no competing financial interest.

■ ACKNOWLEDGMENTS

We thank the ANR (07-BLAN-0287) and the FRM (DCM20111223038) for financial support and grants for D.D. and V.Y.P. We thank Prof. Alexander Demchenko and Dr. Jennifer Wytko for their fruitful comments and critical reading of the manuscript.

■ REFERENCES

- (1) For reviews, see: (a) Wilson, J. N.; Kool, E. T. *Org. Biomol. Chem.* **2006**, *4*, 4265–4274. (b) Sinkeldam, R. W.; Greco, N. J.; Tor, Y. *Chem. Rev.* **2010**, *110*, 2579–2619. (c) Srivatsan, S. G.; Sawant, A. *Pure Appl. Chem.* **2011**, *83*, 213–232. (d) Dai, N.; Kool, E. T. *Chem. Soc. Rev.* **2011**, *40*, 5756–5770.
- (2) (a) Ward, D. C.; Reich, E.; Stryer, L. *J. Biol. Chem.* **1969**, *244*, 1228–1237. (b) Rachofsky, E. L.; Osman, R.; Ross, J. B. *Biochemistry* **2001**, *40*, 946–956.
- (3) Dual emission and ratiometric measurement are commonly obtained with doubly labeled ODNs (e.g., FRET, excimer).^{1d} Few examples with singly labeled ODNs are known. For ODNs labeled with pH-sensitive or charge-transfer dyes, see: (a) Kashida, H.; Sano, K.; Hara, Y.; Asanuma, H. *Bioconjugate Chem.* **2009**, *20*, 258–265. (b) Okamoto, A.; Tainaka, K.; Nishiza, K.; Saito, I. *J. Am. Chem. Soc.* **2005**, *127*, 13128–13129.
- (4) (a) Demchenko, A. P. *FEBS Lett.* **2006**, *580*, 2951–2957. (b) Demchenko, A. P.; Klymchenko, A. S.; Pivovarenko, V. G.; Ercelen, S.; Duportail, G.; Mély, Y. *J. Fluoresc.* **2003**, *13*, 291–295.
- (5) (a) Das, R.; Klymchenko, A. S.; Duportail, G.; Mély, Y. *Photochem. Photobiol. Sci.* **2009**, *8*, 1583–1589. (b) Chou, P. T.; Martinez, M. L.; Clements, J. H. *J. Phys. Chem.* **1993**, *97*, 2618–2622. (c) Hsieh, C.-C.; Jiang, C.-M.; Chou, P.-T. *Acc. Chem. Res.* **2010**, *43*, 1364–1374.
- (6) (a) Demchenko, A. P. *Trends Biotechnol.* **2005**, *23*, 456–460. (b) Demchenko, A. J. *Fluoresc.* **2010**, *20*, 1099–1128.

- (7) (a) Demchenko, A. P.; Mely, Y.; Duportail, G.; Klymchenko, A. S. *Biophys. J.* **2009**, *96*, 3461–3470. (b) Shynkar, V. V.; Klymchenko, A. S.; Kunzelmann, C.; Duportail, G.; Muller, C. D.; Demchenko, A. P.; Freyssinet, J.-M.; Mely, Y. *J. Am. Chem. Soc.* **2007**, *129*, 2187–2193. (c) Shvadchak, V. V.; Klymchenko, A. S.; de Rocquigny, H.; Mély, Y. *Nucleic Acids Res.* **2009**, *37*, No. e25. (d) Yushchenko, D. A.; Fauerbach, J. A.; Thirunavukkuarasu, S.; Jares-Erijman, E. A.; Jovin, T. M. *J. Am. Chem. Soc.* **2010**, *132*, 7860–7861.
- (8) Spadafora, M.; Postupalenko, V. Y.; Shvadchak, V. V.; Klymchenko, A. S.; Mély, Y.; Burger, A.; Benhida, R. *Tetrahedron* **2009**, *65*, 7809–7816.
- (9) Guckian, K. M.; Schweitzer, B. A.; Ren, R. X. F.; Sheils, C. J.; Paris, P. L.; Tahmassebi, D. C.; Kool, E. T. *J. Am. Chem. Soc.* **1996**, *118*, 8182–8183.
- (10) (a) Matray, T. J.; Kool, E. T. *J. Am. Chem. Soc.* **1998**, *120*, 6191–6192. (b) Berger, M.; Ogawa, A. K.; McMinn, D. L.; Wu, Y. Q.; Schultz, P. G.; Romesberg, F. E. *Angew. Chem., Int. Ed.* **2000**, *39*, 2940–2942. (c) Singh, I.; Hecker, W.; Prasad, A. K.; Parmar, V. S.; Seitz, O. *Chem. Commun.* **2002**, 500–501. (d) Brotschi, C.; Mathis, G.; Leumann, C. J. *Chem.—Eur. J.* **2005**, *11*, 1911–1923.
- (11) Loakes, D. *Nucleic Acids Res.* **2001**, *29*, 2437–2447.
- (12) Ogawa, A. K.; Abou-Zied, O. K.; Tsui, V.; Jimenez, R.; Case, D. A.; Romesberg, F. E. *J. Am. Chem. Soc.* **2000**, *122*, 9917–9920.
- (13) (a) Asseline, U.; Delarue, M.; Lancelot, G.; Toulmé, F.; Thuong, N. T.; Montenay-Garestier, T.; Hélène, C. *Proc. Natl. Acad. Sci. U.S.A.* **1984**, *81*, 3297–3301. (b) Amann, N.; Huber, R.; Wagenknecht, H.-A. *Angew. Chem., Int. Ed.* **2004**, *43*, 1845–1847.
- (14) (a) Köhler, O.; Jarikote, D. V.; Singh, I.; Parmar, V. S.; Weinhold, E.; Seitz, O. *Pure Appl. Chem.* **2005**, *77*, 327–338. (b) Wenge, U.; Wagenknecht, H.-A. *Synthesis* **2011**, 502–508. (c) Sinkeldam, R. W.; Marcus, P.; Uchenik, D.; Tor, Y. *ChemPhysChem* **2011**, *12*, 2260–2265.
- (15) Wilson, J. N.; Cho, Y.; Tan, S.; Cuppoletti, A.; Kool, E. T. *ChemBioChem* **2008**, *9*, 279–285.
- (16) (a) Ben Gaied, N.; Glasser, N.; Ramalanjaona, N.; Beltz, H.; Wolff, P.; Marquet, R.; Burger, A.; Mély, Y. *Nucleic Acids Res.* **2005**, *33*, 1031–1039. (b) Kenfack, C. A.; Piemont, E.; Ben Gaied, N.; Burger, A.; Mély, Y. *J. Phys. Chem. B* **2008**, *112*, 9736–9745.
- (17) Godet, J.; Mély, Y. *RNA Biol.* **2010**, *7*, 687–699.
- (18) (a) Godet, J.; Ramalanjaona, N.; Sharma, K. K.; Richert, L.; de Rocquigny, H.; Darlix, J.-L.; Duportail, G.; Mély, Y. *Nucleic Acids Res.* **2011**, *39*, 6633–6645. (b) Bourbigot, S.; Ramalanjaona, N.; Boudier, C.; Salgado, G. F. J.; Roques, B. P.; Mély, Y.; Bouaziz, S.; Morellet, N. *J. Mol. Biol.* **2008**, *383*, 1112–1128.
- (19) (a) Beltz, H.; Azoulay, J.; Bernacchi, S.; Clamme, J. P.; Ficheux, D.; Roques, B.; Darlix, J. L.; Mély, Y. *J. Mol. Biol.* **2003**, *328*, 95–108. (b) Egele, C.; Schaub, E.; Ramalanjaona, N.; Piemont, E.; Ficheux, D.; Roques, B.; Darlix, J. L.; Mély, Y. *J. Mol. Biol.* **2004**, *342*, 453–466. (c) Heilman-Miller, S. L.; Wu, T.; Levin, J. G. *J. Biol. Chem.* **2004**, *279*, 44154–44165.
- (20) Avilov, S. V.; Piemont, E.; Shvadchak, V.; de Rocquigny, H.; Mély, Y. *Nucleic Acids Res.* **2008**, *36*, 885–896.